

An integrated geophysical study east of the southern Chagos Laccadive Ridge Complex, Central Indian Ocean Basin: Implications for the Rodriguez Triple Junction dynamics in the Late Cretaceous

Maria Ana Desa*, T. Ramprasad and K. A. Kamesh Raju

Geological Oceanography, CSIR-National Institute of Oceanography, Dona Paula, Goa 403004 India

*Corresponding author: mdesa@nio.org; Tel: +91 832 2450428; Fax: +91 832 2450602

Abstract

The Central Indian Ocean Basin, east of the southern Chagos Laccadive Ridge complex has evolved due to seafloor spreading in the N-S direction since the Late Cretaceous. The trace of the Rodriguez Triple Junction (RTJ) has been inferred in this basin, but its exact location and dynamics prior to C29o are not known. About 20,000 km of total magnetic intensity data along with satellite gravity mosaic were used to understand the dynamics of the RTJ in the Late Cretaceous.

Synthetic seafloor spreading models endorse the presence of Late Cretaceous to early Palaeogene magnetic anomalies C34y to C24o in the study area. Half-spreading rates are initially low (32 mm/yr) between C34y to C33y, and increase up to 78 mm/yr by C28y. Thereafter a decreasing trend is seen (57 mm/yr). Towards the west in the study area, higher spreading rates (120 mm/yr) between C33y and C32ay, and distorted anomalies between chrons C32ay and C30y are observed. Detailed geophysical analysis suggests that the higher spreading rates are due to the presence of transferred crust, and the distorted anomalies are caused by the presence of fragmented tectonic blocks depicting microplate formation and rotation.

Plate reconstruction models suggest that the RTJ at C34y time lay southwest of Comorin Ridge which coincided with the northern edge of the Conrad Rise. Until C33y, the RTJ left a linear trace parallel to the fracture zone trend on both the Indian and Antarctic plates, while it gradually moved eastwards on the African plate. The RTJ migrated westwards until C31y causing the transfer of a considerable amount of crust from the African plate to both the Indian and Antarctic plates. Thereafter, the RTJ rapidly reversed its migration direction towards the east until C29o causing the formation and rotation of a microplate on the Indian plate and lengthening of the Southwest Indian Ridge.

The present study suggests that this episodic migration of the RTJ may be due to ridge propagation under the influence of the Marion hotspot which was in the vicinity during that period. This RTJ migration resulted in microplate formation, lithospheric transfer and thickened lithosphere similar to the inferences made at many triple junctions in the Pacific Ocean. Thus the origin of anomalous structures such as the Crozet Bank may be related to triple junction dynamics under the influence of Marion hotspot. Further, the counter clockwise rotation of the Southwest Indian Ridge between C33y and C29y may have a causal link with the formation and rotation of the microplate, which occurred during the same period. The present study thus facilitated the inference of the dynamics of the RTJ trace between C34y and C29o on the three plates.

Keywords: Central Indian Ocean Basin, Rodriguez Triple Junction; microplate; Southwest Indian Ridge; episodic migration; Marion hotspot

1. Introduction

The present-day Indian Ocean (Fig. 1) is characterised by an inverted Y-shaped mid-oceanic ridge system (Mckenzie and Sclater, 1971; Schlich, 1982). The Central Indian Ridge (CIR) separating Somalia and Capricorn plates, is a slow spreading ridge with complex geometry due to NNE to NE trending fracture zones (Fisher et al., 1971; Kamesh Raju et al., 2012). The Southwest Indian Ridge (SWIR) separating Somalia and Antarctic plates, is an ultra-slow spreading center with rough topography and large offset fracture zones (Sclater et al., 1981; Fisher and Sclater, 1983; Royer et al., 1988; Bernard et al., 2005). The third arm of the mid-oceanic system is the Southeast Indian Ridge (SEIR) which separates the Capricorn plate from the Antarctic plate and has comparatively higher half-spreading rates of ~30 mm/yr (Small et al., 1999). The above three arms of the Indian mid-oceanic ridge system converge at the Indian Ocean Triple Junction also called the Rodriguez Triple Junction (RTJ) located at 25.5°S and 70°E (Fisher et al., 1971; Mckenzie and Sclater, 1971; Schlich, 1982; Munsch and Schlich, 1989; Dymant, 1993).

The Indian Ocean is characterized with several basins (Fig. 1) such as the Arabian Sea, Bay of Bengal, Mascarene, Mozambique, Madagascar, Crozet, Somali and Central Indian Ocean basins (Mckenzie and Sclater, 1971; Schlich, 1982). The Central Indian Ocean Basin (CIOB) extends from the CIR to the Ninetyeast Ridge and is bounded by the SEIR towards the south.

The CIOB (Fig. 1) has experienced considerable lithospheric deformation over the last 20 Ma (Weissel et al., 1980; Royer and Chang, 1991). The resultant N-S shortening is indicated by the presence of E-W striking topographic undulations of relief of ~1 km and wavelengths of 100-300 km, and 30-80 mgals gravity anomalies (Geller et al., 1983; Sandwell et al., 2014). This deformation resulted in the formation of three plates, i.e., Indian, Capricorn and Australian plates from the single Indo-Australian plate (Royer and Gordon, 1997). Plate reconstructions revealed that the convergence inferred between India and Capricorn due to deformation, could shift a point near 80°E about 30 km to the north (DeMets et al., 2005). Likewise, Africa can be divided into Nubia, Lwandle and Somalia plates (Horner-Johnson et al., 2007), but their motions with respect to the Antarctic plate are recent and small enough to be neglected.

Previous studies have suggested that the ocean floor belonging to the CIOB is devoid of any major topographic features, and the underlying oceanic crust has evolved due to an E-W spreading ridge at relatively higher spreading rates from the Late Cretaceous to Middle Eocene (Mckenzie and Sclater, 1971; Sclater and Fisher, 1974; Schlich, 1982; Kamesh Raju and Ramprasad, 1989). Several N-S

trending fracture zones (FZ) have been inferred based on the magnetic anomaly offsets and gravity signatures (Mckenzie and Sclater, 1971; Patriat and Segoufin, 1988; Kamesh Raju, 1993).

The trace of the RTJ, a suture between the crusts created at the corresponding ridges has been proposed in the CIOB (Fig. 1) based on the presence of conjugate fracture zones, i.e. southern and northern Boussole FZs on either side of CIR, and southern and northern Astrolabe FZs on either side of SEIR (Patriat and Segoufin 1988). Magnetic anomalies C29n through C20n identified on both sides of the three spreading axes were used to locate the trace between these conjugate FZs in the CIOB. Further, it was suggested that the RTJ lay in eastern Mascarene Basin between anomalies C33 and C30, and migrated eastward rapidly from C29n to C21n (Dyment, 1993).

Prior to C29o, the RTJ trace on the Indian plate (Fig. 2) is seen having a westward trend (Patriat and Segoufin, 1988; Dyment, 1993) in contrast to the continuing ~N-S trend inferred by Cande et al. (2010). Additionally, the RTJ has been located at various locations in the CIOB for different times by several authors (e.g., Norton and Sclater, 1979; Bernard et al., 2005; Shuhail et al., 2018). Further, despite the existence of sufficient geophysical datasets, the RTJ trace has not been demarcated on the three plates (India, Antarctica and Africa) for times older than C29o. This major void prompted us to compile all the published data in the form of magnetic picks and fracture zones, and integrate it with the new magnetic data acquired in the CIOB to infer the location of the RTJ trace on the three plates prior to C29o.

The present study integrates the magnetic anomaly identifications made on the new magnetic data with those published in the CIOB. Towards the west in the study area, detailed analysis of the geophysical data indicates the presence of transferred crust and a rotated microplate. Plate reconstruction models thus generated enabled us to trace the RTJ between C34y and C29o. Further, the models suggest that episodic migration of the RTJ occurred from C33y to C29o due to ridge propagation under the influence of the Marion hotspot, leading to microplate formation and emplacement of anomalous structures such as the Crozet Bank.

1.1 Rodriguez Triple Junction

Mckenzie and Sclater (1971) were the first to discuss the dynamics of the RTJ and termed it as a stable ridge-ridge-ridge (RRR) type. Subsequently, the major fracture zones and the axial valleys were mapped by Tapscott et al. (1980) who supported the concept of a stable RRR configuration which has remained mostly unchanged for the last 10 million years. Patriat and Courtillot (1984) suggested that episodic spreading and rift propagation lead to alternate spreading segment and transform fault formation along the SWIR, causing RRR or RRF (ridge-ridge-fault) modes of the RTJ. The RTJ is

inferred to have jumped every one million years creating the ten 70 km spaced easternmost fracture zones of the SWIR (Dyment, 1993).

The decreasing age of the oldest magnetic anomalies on either side of SWIR towards the east is attributed to the rapid eastward migration of the RTJ. After C26n, the RTJ migration slowed down, and is now migrating at 30 km/Ma (Royer et al., 1988). The differences in axes direction and lengthening rates of SEIR and CIR, and spreading asymmetry determine the RTJ configuration since 20 Ma (Honsho et al., 1996; Mendel et al., 2000).

Triple junctions usually leave continuous linear traces marking their path through space and time. The traces between SEIR and SWIR, and between SWIR and CIR are prominent topographic lineations having a large change in strike over a short distance (Patriat and Segoufin, 1988). The third trace between the CIR and SEIR on the Indian plate is mostly devoid of any significant gravity and topographic signatures, and its presence in the CIOB was concluded by the presence of conjugate fracture zones and magnetic anomaly identifications younger than C29n (Patriat and Segoufin 1988; Kamesh Raju and Ramprasad, 1989; Dyment, 1993).

1.2 Study Area

The study area (Fig. 1) is located in the CIOB between longitudes 71°E and 82°E, and latitudes 10°N and 13°S. Crustal age studies indicate that this region has formed between 50 and 90 Ma (Royer et al., 1989; Muller et al., 2016). Prominent N-S trending fracture zones (Vishnu, Indira, northern Boussole and northern Astrolabe FZs) are inferred in this region (Mckenzie and Sclater, 1971; Patriat and Segoufin, 1988; Dyment, 1991). Towards the north, the shallow topography belongs to the Laccadive Basin and the Comorin Ridge. Towards west in the study area, the ~N-S trending shallow, rugged topography belongs to the Chagos Laccadive Ridge (CLR) complex (Fig. 1) extending from ~10°S to 15°N latitudes (Heezen and Tharp, 1964). The origin of the CLR complex has been attributed to Reunion hotspot volcanism (e.g., Duncan, 1990; Torsvik et al., 2013; Ashwal et al., 2017). The study area in general, has flat topography with water depths reaching to >5000 m towards the south. E-W trending, alternate shallow and deep zones towards the east are the manifestations of lithospheric deformation (Geller et al. 1983).

Immediate east of the CLR, between 8°S and 1°N, a strong linear negative gravity anomaly (Fig. 2) is associated with the Vishnu FZ. This fracture zone was considered as a transform segment connecting the magnetic anomalies in the Arabian Sea to those in the CIOB (Mckenzie and Sclater, 1971). It was later found to be conjugate of the Mauritius FZ which defines the southeastern limit of the Mascarene Basin (Norton and Sclater, 1979). The Northern Boussole FZ, also known as 73°E FZ lies east of the

Vishnu FZ (Patriat and Segoufin, 1988; Kamesh Raju, 1993). The Northern Astrolabe FZ also called the Indrani FZ (Mckenzie and Sclater, 1971) lies along 79°E (Patriat and Segoufin, 1988).

Part of the study area (Fig. 1) lies in the Indian Ocean deformation zone, and the relative plate velocity of the motion across its diffuse plate boundary has been up to 6 mm/yr (Gordon et al. 1998). The potential effect of this deformation on the rotation poles was considered minimal and hence ignored in their rotations (Cande and Patriat, 2015). Today, the RTJ is the meeting point of the Somalia, Capricorn, and Antarctic plates, but since the present study deals with the evolution and dynamics of the Late Cretaceous to early Paleogene crust when the Somalia and Capricorn plates were non-existent, we have chosen to term the plates meeting at the RTJ as India, Africa and Antarctica.

The previously inferred RTJ trace in the CIOB enabled its division into the Western and Eastern CIOB (Patriat and Segoufin, 1988). The Western CIOB comprises the oceanic crust formed at the India-Africa plate boundary along the CIR and is conjugate of the Madagascar Basin, while the Eastern CIOB formed at the India-Antarctica plate boundary along the SEIR is the conjugate of the Crozet Basin. These conjugate basins have been investigated in the present study, and the published magnetic picks and fracture zones have been used to infer the RTJ trace prior to C29o time.

Oceanic basins

The Crozet Basin lies between the SWIR in the west and Kerguelen Plateau in the east; the Conrad Rise towards the south and the SEIR towards the north (Fig. 1). The northern Crozet Basin has formed due to the NW-SE striking SEIR since ~45 Ma. Late Cretaceous to Tertiary magnetic anomalies (C34n through C22n) were identified in the southern Crozet Basin (Schlich, 1982), with age decreasing towards the north. These anomalies are right-laterally offset by several N28°E trending FZs, whose orientation changes to N36°E in the southernmost part of the basin. The southern Astrolabe FZ, east of Crozet Plateau is the conjugate to the northern Astrolabe FZ in the eastern CIOB (Patriat and Segoufin, 1988).

Madagascar Basin lies immediate southeast of Mascarene Basin with the Mauritius FZ as its northwest boundary (Fig. 1). It is bounded by the SWIR towards the southeast, the Madagascar Plateau towards the southwest, and the CIR towards the northeast. The magnetic anomaly sequence C30n through C19n inferred in this basin is divided into two segments by the southern Boussole FZ, which runs parallel to and south of Mauritius FZ (Schlich, 1982). The southern Boussole FZ is conjugate to the northern Boussole FZ, while the Mauritius FZ is considered conjugate to the Vishnu FZ (Norton and Sclater, 1979; Patriat and Segoufin, 1988; Dyment, 1993).

Volcanic plateaus

Madagascar Plateau is an N-S elongated feature located south of Madagascar Island (Fig. 1). Based on the difference in the nature of the crust, the Madagascar Plateau is divided along 32°S, into a northern domain and a southern domain (Goslin et al., 1981; Schlich, 1982). The northern domain showing complex seafloor and basement topography, and short wavelength magnetic anomalies is associated with anomalous crust having neither purely continental nor oceanic affinity. The southern domain corresponds to a much-subdued topography, with the Moho lying at about 14 km below the sea level. It is suggested that the southern domain of the Madagascar Plateau and the Crozet Plateau have been created simultaneously, and were later separated by spreading along the SWIR (Goslin et al., 1981).

The Crozet Plateau is composed of two distinct highs, the Del Cano Rise to the west and the Crozet Bank to the east (Fig. 1). The relatively shallow Crozet Bank consisting of five volcanic islands is considered the surface expression of the Crozet plume (Recq et al., 1998). The Crozet Bank is emplaced off-axis on older and cooler lithosphere around C32n (Goslin and Patriat, 1984), while the Del Cano Rise is formed near the SWIR axis around anomaly C24n. The plateau is associated with a regional geoid high and a deep low-velocity zone (Sauter et al., 2009; Breton et al., 2013), suggesting the presence of a significant mantle thermal anomaly below it. However, the source of volcanism of the Crozet Plateau remains a mystery, due to lack of a well preserved prominent volcanic record on the adjacent African, Antarctic and Australian plates that could link the present-day Crozet Plateau to a precursor flood basalt province.

Marion hotspot

The Marion hotspot has been considered fixed at ~46°S for the last 90 Ma (Torsvik et al., 1998; Meert and Tamrat, 2006). In contrast, using moving Indian Ocean hotspot reference frame, about 7° southward motion of the Marion hotspot has been proposed for the same period (O'Neill et al., 2003). The ridge bathymetry anomaly from the Madagascar Plateau to the SWIR has been considered as the track of the Marion hotspot (Duncan and Richards, 1991). The Del Cano Rise might have been created by the Marion hotspot activity (Coffin and Eldholm, 1994). Marion hotspot activity has been divided into three main phases: interaction with the RTJ between 73.6Ma (C33y) and 68.5 Ma (C31o), interaction with the SWIR from 68.5 to 42.7 Ma (C20y), and intraplate volcanism from 42.7 to 0 Ma (Zhang et al., 2011). The motion of the Marion hotspot since 91 Ma has been modelled by Doubrovine et al. (2012).

2. Data and Methodology

About 17,400 km of magnetic data collected in the 1980s under the Polymetallic Nodules (PMN) project has been used in the present study (Table 1). This dataset consists of nine ~N-S to NNW-SSE trending tracks of high quality unpublished magnetic data. In addition, about 2600 km of magnetic data was used from the National Centers for Environmental Information (NCEI), Colorado (Fig. 2). Magnetic picks from published literature have also been used (e.g., Royer et al., 1989; Desa et al., 2009; Cande et al., 2010; Cande and Patriat, 2015). Fracture zones (Wessel et al., 2015; Matthews et al., 2016a), satellite-derived gravity (Sandwell et al., 2014) and world topography grid (Amante and Eakins, 2009) have been used in addition to the large igneous provinces delineated by Coffin and Eldholm (1994), to understand the major evolutionary tectonics.

Analysis of magnetic data constitutes identification of magnetic anomalies and estimation of seafloor spreading parameters using a geomagnetic polarity time scale. Several recently updated geomagnetic polarity times scales are available which differ in their reversal timings based on the source parameters used (e.g., Gee and Kent, 2007; Gradstein et al., 2012). We have done seafloor spreading modelling using these two time scales and found that the identifications remain the same with a slight difference in the inferred spreading rates. We have selected the time scale by Gee and Kent (2007) as it is used by Matthews et al. (2016a), on whose global plate motion model we have built our plate reconstruction models. Table 2 lists the ages of the magnetic chrons used in the present study.

Synthetic seafloor spreading models (Table 3; Fig. 3) were generated for two profiles, one towards the east and the other towards the west of CIOB, to identify the magnetic anomalies using the ‘stripe’ Fortran program of Dan McKenzie. The synthetic models were also generated using MODMAG program (Mendel et al., 2005), and are provided in the supplementary information. We note here that the N-S shortening due to deformation affects the spreading rates by ~2 mm/yr (Gordon et al., 1998), which is less than one-tenth of the prevailing spreading rates; hence we ignore its effect on our seafloor spreading models.

Based on the correlation of the observed magnetic anomalies with the model, magnetic anomaly identifications were made, and spreading rates were inferred. Further, these anomalies were identified on all the profiles used in the present study (Fig. 4). Any deviations in the shape and amplitude of the identified anomalies, any anomalous peaks, and changes in distance between the identified anomalies were noted for further detailed investigation. The magnetic anomaly identifications were then plotted on to the track map along with the published magnetic picks, to understand the evolution of the underlying oceanic crust (Fig. 5).

The higher spreading rates (Fig. 3) and lack of a clear cut correlation between the model and the magnetic profiles towards the west (Fig. 4), prompted us to minutely examine all the geophysical datasets including the updated satellite gravity mosaic (Sandwell et al., 2014) in the study area. These datasets were critically examined for any atypical signatures such as repetition of magnetic anomalies, large gravity variations, etc. Symmetric magnetic anomalies about a central anomaly associated with a gravity low, (Fig. 6a) were attributed to the presence of transferred crust and an extinct spreading center, as done earlier by Jonas et al. (1991). Distorted magnetic signatures associated with complex circular gravity pattern (Fig. 6b) were credited to a rotated microplate, as inferred by Matthews et al. (2016b).

The magnetic picks inferred in this study along with published magnetic isochrons and fracture zones in the CIOB, and the conjugate basins (Madagascar and Crozet Basins), were used as constraints (Royer et al., 1989; Bernard and Munsch, 2000; Desa et al., 2009; Cande et al., 2010; Cande and Patriat, 2015; Matthews et al., 2016a) to generate plate reconstruction models at various chrons. The plate rotation parameters were estimated using the Hellinger tool of the Gplates software (Boyden et al., 2011). This tool is based on the method of Hellinger (1981), and the statistical techniques of Chang (1987) and Royer and Chang (1991). We pursued in detail the methodology followed by Cande and Patriat (2015) without considering the deformation effect in the CIOB, and obtained uncertainty ellipses and the statistical parameter k (Table 4). Rotation poles were also obtained taking into consideration the effect of deformation in the CIOB (Table 5). Further, these rotation poles were compared with other published poles (Royer et al., 1988; Royer and Sandwell, 1989; Cande et al., 2010; Cande and Patriat, 2015; Matthews et al., 2016a) (Table 5, Figure 7)

The computed rotation poles (Tables 4 & 5) were then used to generate the plate reconstruction models using the Gplates software (Boyden et al., 2011). Alternate models were generated, with and without taking into consideration the effect of deformation in the CIOB. Since there are no major changes relevant to our inferences in the resultant models, we have considered the reconstructions based on the most recent global model of Matthews et al. (2016a) which include the deformation effect, for further analysis. This model uses the global moving hotspot reference frame by incorporating the relative motion between the Pacific and Indo-Atlantic hotspots (O'Neill et al. 2005; Doubrovine et al., 2012). As mentioned earlier, we have considered the three plates meeting at the RTJ as India, Africa and Antarctica, and have kept Antarctica in the present day position (Fig. 8).

Four models from chrons C34y and C29o were generated to trace the evolutionary history of the study area, and the dynamics of the RTJ in particular (Table 5; Fig. 8). Further, the visual fit of the magnetic picks on either side of the spreading axis, and the alignment of the conjugate fracture zone trends were

incorporated to refine these models. The offsets in the magnetic anomalies not associated with any known FZs were linked to the RTJ as done in earlier studies (Patriat and Segoufin, 1988; Dymant, 1993). The Marion hotspot locations (Dobrovine et al., 2012) were taken into consideration to infer its role in the dynamics of the RTJ.

The reconstruction models were used to infer the RTJ location at different times, and the timing and mode of formation of the various anomalous structures such as transferred crust and microplate. Further, the inferred locations of the RTJ trace on the three plates were compared with the earlier published traces, and its dynamics during the early evolution of the Indian Ocean were deduced (Fig. 9).

3. Results

Detailed examination of the magnetic data indicates the presence of high-frequency magnetic anomalies towards the west over the CLR complex (e.g., profiles f1, f3, f5) (Fig. 2). Towards the east and south, the magnetic anomalies are the typical seafloor spreading type. Synthetic seafloor spreading model studies (Fig. 3) facilitated the identification of Late Cretaceous to early Palaeogene magnetic anomalies C34y to C26y with half-spreading rates between 32 and 120 mm/yr.

Model studies indicate that the eastern profile 'inmd' depicts excellent correlation with the model despite the uneven bathymetry (Fig. 3) which is the effect of deformation as mentioned earlier. Initially, the half-spreading rate is low, i.e., 35 mm/yr between C34y and C33o. Thereafter the rates increase gradually to 76 mm/yr until C28y and drop to 62 mm/yr by C27y. The western profile 'f6' shows high-frequency magnetic anomalies associated with shallow, rugged topography between C34y and C30y. Nevertheless, the magnetic anomalies can be identified without much difficulty. Half-spreading rate is 32 mm/yr between C34y and C33y, and it increases abruptly up to 120 mm/yr until C32ay. Thereafter it falls to 44 mm/yr and attains values similar to profile inmd.

Figure 4 depicts a fairly good correlation of the magnetic anomalies along all the profiles. The magnetic anomalies younger than C29o depict their perfect signatures on all the profiles. The older anomalies (C34y to C29o) were confidently identified on most of the profiles towards the east, and tentatively identified on some of the profiles towards the west. The distorted magnetic signatures seen on some of the western profiles reflect complex tectonic activity, which is described in detail later.

The satellite gravity mosaic depicts several ~N-S trending lineations, most of which are the fracture zones (Fig. 5). Towards the north, relatively positive NW-SE trending gravity signature belongs to the Comorin Ridge. Immediate east of the complex positive signature of the CLR complex is the steep linear gravity low of the Vishnu FZ. Zones of alternate positive and negative gravity seen running

roughly E-W towards the east are the signatures of the lithospheric deformation as inferred by Geller et al. (1983).

The disposition of the identified Late Cretaceous to early Palaeogene C34y to C24o magnetic picks (Fig. 5) along with the inferred fracture zones (Matthews et al., 2016a) corroborates that the underlying oceanic crust has evolved due to ~NW-SE to E-W trending spreading center. The anomaly C34y trends NW-SE with right lateral offsets east of 75°E. A large offset of the C34y isochrons in the absence of a known fracture zone is seen at the southwestern edge of the Comorin Ridge (~78.5°E). WNW-ESE trending and right lateral offsetting gravity lineations and topographic peaks are seen along the C34y isochrons between 75.5° and 77.5°E (Figs. 4 & 5). The anomalies C33o and C33y also depict NW-SE trend with a major offset devoid of any known fracture zone along ~78.5°E. A point to note is the C33y and C32ay isochrons lying adjacent to each other along 3°S, west of northern Astrolabe FZ (encircled in figure 5). Further south, the younger anomalies trend roughly E-W. The northern Boussole FZ offsets the magnetic anomalies younger than C31y right laterally by about 160 km. The other FZs (northern Astrolabe, Indira, etc.) also offset the anomalies right laterally.

Profile f6 having variable spreading rates and distorted magnetic anomalies older to C30y (Fig. 3), prompted us to do a detailed examination of the magnetic data along the western profiles (Fig. 4). Phase shifting of these anomalies (Schouten and McCamy, 1972) indicated that these anomalies are associated with a high degree of anomalous skewness. Additional anomalies are seen between C33y and C32ay along three profiles, which are responsible for the high spreading rates (Fig. 6a). These anomalies are a mirror image of the adjacent pre-existing anomalies forming a set of symmetric magnetic anomalies about a central anomaly. In this zone, the bathymetry also depicts a mirror image with a scarp at the southern edge. A prominent gravity low is seen at the central magnetic anomaly, and smaller gravity lows are seen on either edge of this zone. These symmetric magnetic anomalies about a central anomaly associated with a gravity low, are attributed to the presence of transferred/extra crust and an extinct spreading center (Jonas et al., 1991). Thus the presence of transferred crust, about 220 km wide in the E-W direction and up to 120 km in the N-S direction could be traced around 2°S in the western CIOB based on the magnetic anomalies and gravity signature (Fig. 6b). The presence of this transferred crust reduces the large offset of the older anomalies seen along 78.5°E, and changes the anomaly trend from NW-SE to E-W.

Likewise, C31o signature appears distorted along the same three profiles suggesting a change in the mode of formation/nature of the underlying crust probably due to some complex tectonics (Fig. 6a). The gravity signature over these distorted C31o anomalies (between 4°S and 5°S) depicts circular discontinuous trends (Fig. 6b). These circular trends probably indicate microplate formation and

subsequent block rotation. The inferred microplate has a diameter of about 180 km. The profile f3 depicts even more complex geophysical signatures (Fig. 6a). The transferred crust and the rotated block have been tentatively interpreted on this profile, too.

3.1 Plate reconstruction models

The rotation pole parameters obtained in this study using the Hellinger method (Table 4) without incorporating deformation effect are in general similar to those of Cande and Patriat (2015), and depict small error ellipses except for the C33y of India-Antarctica rotation (Fig. 7). We mention here that this C33y rotation pole (8.81, 12.49, -56.42) did not yield a good plate reconstruction model either. Based on the visual fit of the magnetic picks and the alignment of the conjugate fracture zone trends, this pole was modified (9.15, 12.72 -56.49), while generating the plate reconstruction model.

For the India-Antarctica rotation, the poles inferred without taking into consideration the deformation effect differ considerably from those estimated after incorporating the deformation effect (Tables 4 & 5, Fig. 7a). The Royer and Sandwell (1989) rotation poles diverge slightly, while the Matthews et al. (2016a) poles which incorporate the deformation effect lie towards the northwest.

For the Africa-Antarctica spreading, all the rotation poles depict a fairly good match for C34y (Fig. 7b). Matthews et al. (2016a) rotation poles for C33y, C31y and C29o differ considerably from the other poles.

Figure 8 depicts the reconstruction models generated based on the global model of Matthews et al. (2016a) taking into account the deformation effect (Table 5). A good fit of the magnetic picks on either side of the spreading axis and a clear match in the conjugate fracture zone trends are observed.

The C34y (83 Ma) reconstruction (Fig. 8a) depicts that the C34y picks of the CIOB lie between the Northern Madagascar Plateau and the Kerguelen-86°E FZ. One sees that the C34y picks on the western side of the study area (i.e., between 75.5° and 78.5°E, in Fig. 5) cannot be superimposed on those on the western side of Antarctica (SWIR), while those towards the east match well with their conjugates. Moreover, the authenticity of these picks prompted us to infer that the western picks belong to two different spreading centers, and invoke the presence of a triple junction. Further, the C34y picks in the western CIOB can be connected to those in the Mascarene Basin between Madagascar and India via an unknown transform fault probably lying at the eastern edge of the Northern Madagascar Plateau. Thus the Mascarene Ridge (MR) extending eastward into the western CIOB formed the third arm of the RTJ. The model further suggests that the RTJ may be a RRR type and is located at the southwest corner of Comorin Ridge coinciding with the northern edge of Conrad Rise. This RTJ location is around 78.5°E in the CIOB where we have observed a fairly large offset of the C34y isochrons without

any FZ signature (Figs. 8a & 5). Thus the right lateral offsetting gravity lineations seen in western CIOB are characteristic of the MR and are absent on the SEIR. Further, the MR and SEIR spreading centers do not depict any significant angle between their trends at the RTJ. The model depicts that the volcanic edifices such as Comorin Ridge, the Conrad Rise and the northern Madagascar Plateau existed by this time. As per the model, the location of the Marion hotspot is southeast of Madagascar. Along the SWIR, orthogonal seafloor spreading between Africa and Antarctica is depicted by the SWIR FZs. The C33y (73.6 Ma) reconstruction (Fig. 8b) depicts the continuation of the seafloor spreading along the three arms of the RTJ. The RTJ trace is N-S on both the Indian and Antarctic plates, while on the African plate it is gradually trending eastward. The RTJ appears to be the RRR/RRF type. Minimal obliquity is seen between the MR and SEIR. The model depicts the appearance of the Vishnu FZ by this time offsetting the isochrons east of the Northern Madagascar Plateau. The SWIR is seen gradually lengthening eastward. Further, the model suggests that the Marion hotspot lies beneath the northern Madagascar Plateau.

The C31y (67.7 Ma) picks inferred on either side of the present-day SWIR are strong constraints for this model which depicts northwest propagation of the SWIR causing westward migration of the RTJ (Fig. 8c). This propagation of the SWIR caused lengthening of the SEIR and transfer of crust from the African plate to the other two plates. On the Indian plate, the transferred crust is in the form of the 220 by 120 km extra crust identified using magnetic and gravity data (Fig. 6). The crust transferred on the Antarctic plate includes the older crust generated at the Africa-Antarctica boundary and the older African RTJ trace. On the Antarctic plate, the model depicts that the RTJ migrated rapidly westward encircling the Crozet Bank which has been emplaced by this time (Goslin and Patriat, 1984). The model indicates that the Marion hotspot is in close vicinity of the SWIR and the RTJ. Another point to note is that the western fracture zones of the SWIR are depicting counter clockwise rotation. Based on their coincident timing, one can infer a genetic link between this rotation of the fracture zones and westward RTJ propagation.

The C29o reconstruction (64.7 Ma) depicts the formation of the inferred rotated microplate on the Indian plate (Fig. 8d). The RTJ moved eastward rapidly by encircling the microplate marking an eastward-trending trace on the three plates. Both the MR and SWIR lengthened rapidly at the cost of SEIR. Further, the model depicts that the RTJ is the RRR type, and the MR and SEIR are almost collinear. The curving of the fracture zones in the Africa-Antarctica corridors appears to continue. The Boussole FZ is now active along with the Vishnu FZ, and the present-day Madagascar Basin has started evolving. Further, our model depicts overprinting of the older magnetic isochrons due to Marion hotspot activity.

4. Discussion

The higher half-spreading rates and atypical geophysical signatures towards the west in the study area helped to demarcate the extent of the crust transferred from the African plate. This transferred crust lies around 2°S, is about 220 km wide in the E-W direction and up to 120 km in the N-S direction. Further, the distorted magnetic anomalies and circular discontinuous trends in gravity signature between 4°S and 5°S indicate the presence of a rotated microplate having a diameter of about 180 km (Fig. 6). The distorted magnetic signatures for times older to C31y (Fig. 3, 4 and 6) are in agreement with the reported anomalous skewness of magnetic anomalies caused by spreading ridge reorganisation in the CIOB (Dyment et al., 1994).

The trace of the RTJ in the CIOB between C34y and C29o demarcates the crusts generated at the two spreading centers, MR and SEIR during that period. Due to the almost collinear nature, i.e., similar spreading rates and directions of these spreading centers (Fig. 8), the RTJ trace is less discernible on the Indian plate as inferred earlier (Patriat and Segoufin, 1988; Kamesh Raju et al., 1989; Dyment, 1993). The present study suggests that the RTJ lay at the southwestern edge of the Comorin Ridge at C34y and moved N-S linearly until C33y (Fig. 9a). These locations are east of those inferred in earlier works (e.g., C34y and C33y reconstructions of Bernard et al., 2005). Further, the study suggests that the RTJ moved westward between C33y and C31y, transferring some crust from the African plate to the Indian plate and leaving an E-W trending trace. The RTJ then moved rapidly eastward until C29o encircling the microplate. These dynamics of the RTJ trace are in agreement with the westward trend of the RTJ trace in the CIOB prior to C29o (Patriat and Segoufin, 1988; Dyment, 1993), and the proposition that RTJ lay in eastern Mascarene Basin between anomalies C33 and C30 and migrated eastward rapidly from C29n to C21n (Dyment, 1993).

On the African and Antarctic plates, the RTJ trace between C31y and C29o (Fig. 9b) almost concurs with those inferred in earlier studies (Patriat and Segoufin, 1988; Dyment, 1993). The older RTJ trace on the Antarctic plate is linear between C34y and C33y. The RTJ then migrates rapidly westward by C31y time (Fig. 9b), and we believe this migration has occurred in a circular manner (Fig. 8) as inferred on the Indian plate between C31y and C29o. Here the Crozet Bank may have been emplaced over the probable location of a microplate. Further, the present study suggests that the older RTJ trace is absent on the African plate as it has been transferred to the Antarctic plate (Fig. 8c) and may have been destroyed later due to overprinting.

The present study suggests that the eastern edge of the northern Madagascar Plateau may have acted as a large offset transform fault between the C34y anomalies of the MR and the western CIOB (Fig.

8a). Conversely, the transform fault may have limited/defined the extent of the northern Madagascar Plateau. Such a scenario has been reported along the SWIR (Georgen and Lin, 2003). By C33y, as the SWIR propagated eastward, the Vishnu/Mauritius FZ acted as a major transform fault (Fig. 8b), and the spreading corridor between the Mahanoro and Mauritius FZs evolved. The northwest propagation of the easternmost spreading segment of the SWIR between C33y and C31y, caused the transfer of the crust east of the Mauritius FZ to the Indian plate. Simultaneously, part of the older crust generated at the Africa-Antarctica boundary was transferred to the Antarctic plate resulting in the formation of excess crust southwest of Crozet Bank (Fig. 8c). The presence of excess crust is in agreement with an extinct spreading center (Fig. 9b) proposed by Whittaker et al. (2015). The rapid eastward migration of the RTJ after C31y caused lengthening of the MR, and initiated the formation of the Madagascar Basin by C29o (Fig. 8d). These phenomena explain the absence of anomalies older to C29o in the Madagascar Basin.

Royer et al. (1988) assumed that between C34 and C32, the RTJ was RFF type and remained fixed with respect to Africa causing lengthening of SEIR, while after C32 time, the RTJ became RRF or RRR type and its eastward migration occurred with slow and oblique spreading along the SWIR. In the present study, lengthening of the SEIR occurred due to the westward migration of the RTJ between C33y and C31y, while the rapid eastward migration between C31y and C29o caused lengthening of the SWIR (Fig. 8). The present study is unable to assert the exact type of RTJ at different times, and more geoscientific data is required to determine the same.

4.1 Role of Marion hotspot

The Marion hotspot is attributed for the Late Cretaceous igneous activity (96 – 84 Ma) around Madagascar and southwest India, which ultimately lead to their separation (Storey et al., 1995; Torsvik et al., 2000). The arrival of the RTJ southeast of Madagascar by 92 Ma and its interaction with the Marion hotspot formed the volcanic edifices like northern Madagascar Plateau and Conrad Rise (Diament and Goslin, 1986; Bernard et al., 2005). The inferred locations of the Marion hotspot for the last 90 Ma (Dobrovine et al., 2012) indicate that the hotspot was in a strong position to influence the evolution of the present study area and the RTJ in particular.

Plate reconstructions suggest that by C31y, the Marion hotspot lay in close vicinity of the SWIR causing it to jump northwest resulting in the RTJ moving westward (Fig. 8c). Such interactions of the Marion hotspot with the RTJ and the SWIR are in agreement with those inferred by Zhang et al., (2011). Further, the reconstructions indicate that the Marion hotspot activity caused the older anomalies on the African plate to be wiped out (Fig. 8). The rapid westward migration of the RTJ may

have created a microplate on the Antarctic plate by C31y on par with that visible on the Indian plate, and its deformed/fragmented nature may have been conducive for extrusive volcanism emplacing the Crozet Bank. In the absence of a prominent volcanic trace linking the present-day Crozet Plateau to any precursor flood basalt province, the migrating RTJ interaction with the Marion hotspot seems to be an alternative mode for its formation.

4.2 Counter clockwise rotation of the SWIR

A major change in spreading direction from NNE-SSW to NNW-SSE with a sharp fall in spreading rates has been inferred along the SWIR between C31 and C29 (Patriat et al. 1985; Royer et al. 1988), which caused counter clockwise rotation of the African plate and clockwise rotation of the Antarctic plate. Patriat and Segoufin (1988) inferred the reorganization of RTJ and SWIR in the form of ridge jumps, since C29n. Bernard et al. (2005) used the vertical gradient of satellite gravity data to infer that complex spreading of the SWIR began at C33n contemporaneous with the rapid increase in velocity of India with respect to Antarctica and rapid migration of the RTJ. The SWIR rotations constrain a significant change in the migration path of the Africa–Antarctica stage poles following C33y coincident with the most rapid slowdown in Africa’s motion, and another significant change following C31y coincident with the most rapid acceleration of India’s northward motion (Cande and Patriat, 2015). At C33y, Shuhail et al. (2018) inferred a major reorientation of the spreading system from E-W to NE-SW in the Mascarene Basin, and from ~NW-SE to E-W in the CIOB.

The present study demonstrates that the transfer of oceanic crust from the African to the Indian plate by C31y results in the NW-SE trend of the chrons becoming E-W. The rapid westward and eastward migrations of the RTJ along with the formation and rotation of the microplate between C31y and C29o inferred in the present study, can be linked to the rotations along the SWIR. Moreover, the microplate may have acted as a pivot/pole for these rotations, as well as the spreading direction changes in all the basins of the Indian Ocean.

4.3 Tectonics behind RTJ episodic migration

Ridge propagation into existing seafloor (Hey, 1977) results in captured rigid blocks called microplates which rotate rather independent of the surrounding plates (Mammerickx and Klitgord, 1982). Microplate formation and rotation has been reported in the absence of ridge death due to step-wise migration of a triple junction (Tebbens et al., 1997). Microplate rotation produces ‘circuitous seafloor’ identifiable by circular gravity pattern with alternate negative and positive signatures such as the Mammerickx microplate in the Indian Ocean (Mathews et al., 2016b). The rotated microplate

identified in the present study (Fig. 6) depicting similar gravity signatures may have formed due to RTJ migration as postulated above.

Episodic triple junction migrations have been reported in the Pacific Ocean (Bird et al., 1999) caused by ridge propagation resulting in lithospheric capture and thickening, and microplate formation under the influence of hotspot activity. Further, models depicting how a triple junction migrates in discrete jumps that involve rift propagation leading to microplate formation were generated. In the present study, under the influence of the Marion hotspot, northwest propagation of the easternmost segment of the SWIR occurred from C33y to C31y, resulting in an episodic westward migration of the RTJ which caused the transfer of crust from the African to the other plates, and the emplacement of the Crozet Bank (Fig. 8). The formation of the microplate on the Indian plate between C31y and C29o, can also be attributed to the RTJ dynamics as described by Bird et al. (1999).

5. Conclusions

Detailed analysis of the magnetic data indicated the presence of Late Cretaceous to early Palaeogene anomalies C34y to C24o in the study area. Further, the synthetic seafloor spreading model suggested that seafloor spreading occurred at variable half-spreading rates ranging from 32 to 120 mm/yr in ~N-S direction. The major fracture zones offset the magnetic anomalies right laterally with the northern Boussole FZ offsetting the younger magnetic anomalies by about 160 km.

Based on symmetric magnetic anomaly pattern about a central anomaly associated with a gravity low, the presence of 220 by 120 km transferred crust can be inferred between isochrons C33y and C31y around 2°S in the western CIOB. Just south of it (4 to 5°S), between isochrons C31y and C29o, complex circular gravity signatures associated with distorted magnetic anomalies are seen depicting the presence of a rotated microplate.

Plate reconstruction models suggest that the RTJ at C34y time lay southwest of Comorin Ridge which coincided with the northern edge of the Conrad Rise. Between C33y and C31y, northwest propagation of the SWIR caused episodic westward migration of the RTJ resulting in lithospheric transfer from the African plate to the Indian and Antarctic plates. This westward migration of the RTJ probably occurred in a circular manner around the Crozet Bank on the Antarctic plate. Thereafter, the RTJ migrated eastward causing the formation and rotation of microplate in the CIOB by C29o. The observed rotation of the fracture zones of the SWIR during this same period may have a causal link with the RTJ migration and microplate rotation.

The locations of the RTJ trace between C34y and C29o are inferred on the three plates for the first time. These locations form constraints for future refinement of the early evolutionary history of the

Indian Ocean and the global plate motion models. The trace of the RTJ is linear (N-S) between C34y and C33y on the Indian and Antarctic plates, whereas it shows an eastward trend on the African plate. Between C33y and C29o, circular traces are inferred on the Antarctic and Indian plates due to the westward followed by eastward migration of the RTJ. The RTJ trace on the African plate older to C31y was transferred to the Antarctic plate due to ridge propagation, and is virtually destroyed by overprinting. Hence the RTJ trace older to C31y is absent on the African plate.

The plate models suggest that the third arm of the RTJ continues as the MR between Madagascar and India from C34y to C29o. Due to the almost collinear nature of the MR and the SEIR, i.e., similar rate and direction of spreading, the RTJ trace is less prominent on the Indian plate. The eastward migration of the RTJ since C31y initiated the formation of the Madagascar Basin which explains the absence of anomalies older to C29o in the Madagascar Basin.

The present study suggests that anomalous tectonic structures in the form of a microplate, lithospheric transfer and thickened lithosphere (Crozet Bank) have formed due to episodic migration of the RTJ, under the influence of the Marion hotspot which was in the vicinity during that period.

Acknowledgments

The authors wish to thank the Director, NIO for the necessary permission. They are also grateful to the Department of Ocean Development, New Delhi, India (now Ministry of Earth Sciences (MoES)) for the magnetic data used in the study. The authors are indebted to Dr. Michele Rebesco (Editor-in-Chief, Marine Geology) for his encouragement. Figures are generated using the GMT software (Wessel and Smith, 1998). This is NIO contribution no:

References

- Amante, C., Eakins, B. W., 2009. ETOPO11 Arc-Minute Global Relief Model: Procedures, Data Sources and Analysis. NOAA Technical Memorandum NESDIS NGDC-24, 19.
- Ashwal, L.D., Wiedenbeck, M., Torsvik, T.H., 2017. Archaean zircons in Miocene oceanic hotspot rocks establish ancient continental crust beneath Mauritius. *Nature Communications* doi: 10.1038/ncomms14086
- Bernard, A., Munsch, M., 2000. Were the Mascarene and Laxmi Basins (western Indian Ocean) formed at the same spreading centre? *Comptes Rendus de l'Academie des Sciences-Series IIA, Earth Planetary Science* 330, 777-783.
- Bernard, A., Munsch, M., Rotstein, Y., Sauter, D., 2005. Refined spreading history at the Southwest Indian Ridge for the last 96 Ma, with the aid of satellite gravity data. *Geophysical Journal International* 162, 765-778.
- Bird, R.T., Tebbens, S.F., Kleinrock, M.C., Naar, D.F., 1999. Episodic triple-junction by rift propagation and microplates. *Geology* 27, 911-914.

- Breton, T., Nauret, F., Pichat, S., Moine, B., Moreira, M., Rose-Koga, E.F., Auclair, D., Bosq, C., Wavrant, L-M., 2013. Geochemical heterogeneities within the Crozet hotspot. *Earth and Planetary Science Letters* 376, 126-136.
- Boyden, J. A., Müller, R. D., Gurnis, M., Torsvik, T. H., Clark, J. A., Turner, M., Ivey-Law, H., Watson, R. J., Cannon, J. S., 2011. Next generation Plate-tectonic Reconstructions Using GPlates, in: Keller, G. R., Baru, C. (Eds.), *Geoinformatics: Cyberinfrastructure for the Solid Earth Sciences*. Cambridge University Press, Cambridge, UK, pp. 95–113.
- Cande, S. C., Patriat, P., Dymant, J., 2010. Motion between the Indian, Antarctic and African plates in the early Cenozoic. *Geophysical Journal International* 183,127-149.
- Cande, S. C., Patriat, P., 2015. The autocorrelated velocities of Africa and India in the Late Cretaceous and early Cenozoic. *Geophysical Journal International* 200, 227-243.
- Chang, T., 1987. On the statistical properties of estimated rotations. *Journal of Geophysical Research* 92, 6319–6329.
- Coffin, M.F., Eldholm, O., 1994. Large igneous provinces: crustal structure, dimensions and external consequences. *Reviews of Geophysics* 32, 1-36.
- DeMets, C., Gordon, R.G., Royer, J-Y., 2005. Motion between the Indian, Capricorn and Somalian plates since 20 Ma: implications for the timing and magnitude of distributed lithospheric deformation in the equatorial Indian Ocean. *Geophysical Journal International* 161, 445-468.
- Desa, M., Ramana, M. V., Ramprasad, T., 2009. Evolution of the Late Cretaceous crust in the equatorial region of the Northern Indian Ocean and its implication in understanding the plate kinematics. *Geophysical Journal International* 177, 1265-1278.
- Diamant, M., Goslin, J., 1986. Emplacement of the Marion Dufresne, Lena and Ob seamounts (south Indian Ocean) from a study of isostasy. *Tectonophysics* 121 253-262.
- Dobrovine, P.V., Steinberger, B., Torsvik, T.H., 2012. Absolute plate motions in a reference frame defined by moving hot spots in the Pacific, Atlantic, and Indian Oceans. *Journal of Geophysical Research* 117, doi:10.1029/2011JB009072.
- Duncan, R.A. 1990. The volcanic record of Reunion hotspot, in: Duncan, R.A., Backman, J., et al., (Eds.), *Proceedings of the Ocean Drilling Program, Scientific Results*, 115, College Station, TX (Ocean Drilling Program), pp. 3-10.
- Duncan, R.A., Richards, M.A., 1991. Hotspots, mantle plumes, flood basalts, and true polar wander. *Reviews of Geophysics* 29, 31-50.
- Dymant, J., 1991. Structure et evolution de la lithosphère océanique dans l'océan Indien: apport des anomalies magnétiques. *These de Doctorat, Université Louis Pasteur, Strasbourg*.
- Dymant, J., 1993. Evolution of the Indian Triple Junction between 65 and 49 Ma (Anomalies 28 to 21). *Journal of Geophysical Research* 98, 13863-13877.
- Dymant, J., Cande, S.C., Arkani-Hamed, J., 1994. Skewness of marine magnetic anomalies created between 85 and 40 Ma in the Indian Ocean. *Journal of Geophysical Research* 99, 24121-24134.

- Fisher, R.L., Sclater, J.G., McKenzie, D.P., 1971. Evolution of the Central Indian Ridge, western Indian Ocean. *Geological Society of America Bulletin* 82, 553-562.
- Fisher, R.L., Sclater, J.G., 1983. Tectonic evolution of the southwest Indian Ocean since the Mid-Cretaceous: Plate motions and stability of the pole of Antarctica/Africa for at least 80 myr. *Geophysical Journal of Royal Astronomical Society* 73, 553-576.
- Gee, J.S., Kent, D.V., 2007. Source of oceanic magnetic anomalies and the geomagnetic polarity timescale. *Treatise on Geophysics* 5, 455-507.
- Geller, C.A., Weissel, J.K., Anderson, R.N., 1983. Heat transfer and intraplate deformation in the central Indian Ocean. *Journal of Geophysical Research* 88, 5560-5570.
- Georgen, J., Lin, J., 2003. Plume-transform interactions at ultra-slow spreading ridges: implications for the Southwest Indian Ridge. *Geochemistry Geophysics Geosystems* 4, 9106, doi:10.1029/2003GC000542.
- Gordon, R.G., DeMets, C., Royer, J-Y., 1998. Evidence for long-term diffuse deformation of the lithosphere of the equatorial Indian Ocean. *Nature* 395, 370-373.
- Goslin, J., Patriat, P., 1984. Absolute and relative plate motions and hypothesis on the origin of five aseismic ridges in the Indian Ocean. *Tectonophysics* 101, 221-244.
- Goslin, J., Recq, M., Schlich, R., 1981. Emplacement and evolution of the Madagascar ridge and Crozet submarine plateau. *Bulletin of Society of Geology of France* 23, 609-618.
- Gradstein, F.M., Ogg, J.G., Schmitz, M., Ogg, G., 2012. *The geologic time scale 2012*. Elsevier, 1176 pp.
- Heezen, B. C., Tharp, M., 1964. *Physiographic diagram of the Indian Ocean (with descriptive sheet)*. Geological Society of America, New York.
- Hellinger, S.J., 1981. The uncertainties of finite rotations in plate tectonics. *Journal of Geophysical Research* 86, 9312-9318.
- Hey, R., 1977. A new class of pseudo-faults and their bearing on plate tectonics: a propagating rift model. *Earth and Planetary Science Letters* 37, 321-325.
- Honsho, C., Tamali, K., Fujimoto, H., 1996. Three-dimensional magnetic and gravity studies of the Rodriguez Triple Junction in the Indian Ocean. *Journal of Geophysical Research* 101, 15837-15848.
- Horner-Johnson, B.C., Gordon, R.G., Argus, D.F., 2007. Plate kinematic evidence for the existence of a distinct plate between the Nubian and Somalian plates along the Southwest Indian Ridge. *Journal of Geophysical Research* 112, B05418, doi:10.292006JB004519.
- Jonas, J., Hall, S., Casey, J.F., 1991. Gravity anomalies over extinct spreading centers: A test of gravity models of active centers. *Journal of Geophysical Research* 96, 11759-11777.
- Kamesh Raju, K.A., 1993. Magnetic lineations, fracture zones and seamounts in the Central Indian Basin. *Marine Geology* 109, 195-201.

- Kamesh Raju, K.A., Ramprasad, T., 1989. Magnetic lineations in the Central Indian Ocean for the period A24-A21: A study in relation to the Indian Ocean Triple Junction trace. *Earth and Planetary Science Letters* 95, 395-402.
- Kamesh Raju, K.A., Samudrala, K., Drolia, R.K., Amarnath, D., Ramachandran, R., Mudholkar, A.V., 2012. Segmentation and morphology of the Central Indian Ridge between 3°S and 11°S, Indian Ocean. *Tectonophysics* 554-557, 114-126.
- Mammerickx, J., Klitgord, K.D., 1982. Northern East Pacific Rise: evolution from 25 m.y. B.P. to the present. *Journal of Geophysical Research* 87, 6751–6759.
- Matthews, K. J., Maloney, K. T., Zahirovic, S., Williams, S. E., Seton, M., Müller, R. D., 2016a. Global plate boundary evolution and kinematics since the late Paleozoic. *Global and Planetary Change* doi: 10.1016/j.gloplacha.2016.10.002.
- Matthews, K.J., Muller, R.D., Sandwell, D.T., 2016b. Oceanic microplate formation records the onset of India-Eurasia collision. *Earth and Planetary Science Letters* 433, 204-214.
- McKenzie, D., Sclater, J. G. 1971. The evolution of the Indian Ocean since the Late Cretaceous. *Geophysical Journal of Royal Astronomical Society* 25, 437-528.
- Meert, J.G., Tamrat, E., 2006. Paleomagnetic evidence for a stationary Marion Hotspot: Additional paleomagnetic data from Madagascar. *Gondwana Research* 10, 340-348.
- Mendel, V., Sauter, D., Patriat, P., Munsch, M., 2000. Relationship of the Central Indian Ridge segmentation with the evolution of the Rodrigues Triple Junction for the past 8 Myr. *Journal of Geophysical Research* 105, 16563-16575.
- Mendel, V., Munsch, M., Sauter, D., 2005. MODMAG, a MATLAB program to model marine magnetic anomalies. *Computers and Geosciences* 31, 589-597. 10.1016/j.cageo.2004.11.007.
- Müller, R.D., Seton, M., Zahirovic, S., Williams, S.E., Matthews, K.J., Wright, N.M., Shephard, G.E., Maloney, K.T., Barnett-Moore, N., Hosseinpour, M., Bower, D.J., Cannon, J., 2016. Ocean Basin Evolution and Global-Scale Plate Reorganization Events since Pangea Breakup. *Annual Review of Earth and Planetary Sciences* 44, doi: 10.1146/annurev-earth-060115-012211.
- Munsch, M., Schlich, R. 1989. The Rodriguez Triple Junction (Indian Ocean): Structure and evolution for the past one million years. *Marine Geophysical Research* 11, 1-14.
- Norton, I. O., Sclater, J. G. 1979. A model for the evolution of the Indian Ocean and the breakup of Gondwanaland. *Journal of Geophysical Research* 84, 6803-6830.
- O'Neill, C., Müller, R.D., Steinberger, B., 2003. Geodynamic implications of moving Indian Ocean hotspots. *Earth and Planetary Science Letters* 215, 151-168.
- O'Neill, C., Müller, R.D., Steinberger, B., 2005. On the uncertainties in hotspot reconstructions and the significance of moving hot spot reference frames. *Geochemistry Geophysics Geosystems* 6, Q04003, doi:10.1029/2004GC000784
- Patriat, P., Courtillot, V., 1984. On the stability of triple junctions and its relation to episodicity in spreading. *Tectonics* 3, 317-332.

- Patriat, P., Segoufin, J., Goslin, J., Beuzart, P., 1985. Relative positions of Africa and Antarctica in the Upper Cretaceous: evidence for nonstationary behaviour of fracture zones. *Earth and Planetary Science Letters* 75, 204–214.
- Patriat, P., Segoufin, J., 1988. Reconstruction of the Central Indian Ocean. *Tectonophysics* 155, 235-260.
- Recq, M., Goslin, J., Charvis, P., Operto, S., 1998. Small-scale crustal variability within an intraplate structure: the Crozet Bank (southern Indian Ocean), *Geophysical Journal International* 134, 145-156.
- Royer, J-Y., Chang, T., 1991. Evidence for relative motions between the Indian and Australian plates during the last 20 m.y. from plate reconstructions: Implications for the deformation of the Indo-Australian plate. *Journal of Geophysical Research* 96, 11779-11802.
- Royer, J-Y, Gordon, R.G., 1997. The motion and boundary between the Capricorn and Australian Plates. *Science* 277, 1268-1274.
- Royer, J-Y, Sandwell, D. T., 1989. Evolution of the Eastern Indian Ocean since the Late Cretaceous: constraints from Geosat altimetry. *Journal of Geophysical Research* 94, 13 755–13 782.
- Royer, J-Y., Patriat, P., Bergh, H.W., Scotese, C.R., 1988. Evolution of the Southwest Indian Ridge from the Late Cretaceous (anomaly 34) to the middle Eocene (anomaly 20). *Tectonophysics* 155, 235-260.
- Royer, J-Y., Sclater, J. G., Sandwell, D. T., 1989. A preliminary tectonic fabric chart of the Indian Ocean, in: Brune, J. N., (Ed.), *Proceedings of the Indian Academy of Sciences, Earth and Planetary Sciences* 98, 7-24.
- Sandwell, D.T., Muller, R. D., Smith, W. H. F., Garcia, E., Francis, R., 2014. New global marine gravity model from CryoSat-2 and Jason-1 reveals buried tectonic structure. *Science* 346, 65-67.
- Sauter, D., Cannat, M., Meyzen, C., Bezos, A., Patriat, P., Humler, E., Debayle, E., 2009. Propagation of a melting anomaly along the ultraslow Southwest Indian Ridge between 46°E and 52°20'E: interaction with the Crozet hotspot? *Geophysical Journal International* 179, 687-699.
- Schlich, R., 1982. The Indian Ocean: aseismic ridges, spreading centers and ocean basins, in: Nairn, A. E., Stehli, F. G. (Eds.), *The Ocean Basins and Margins*, Plenum, New York, 6, pp.51-147.
- Sclater, J.G., Fisher, R.L., 1974. Evolution of the east Central Indian Ocean, with emphasis on the tectonic setting of the Ninetyeast Ridge. *Geological Society of America Bulletin* 85, 683–702.
- Sclater, J.G., Fisher, R.L., Patriat, P., Tapscott, C.R., Parsons, B., 1981. Eocene to recent development of the South-west Indian Ridge, as consequence of the evolution of the Indian Ocean Triple Junction. *Geophysical Journal of Royal Astronomical Society* 64, 587-604.
- Schouten, H., McCamy, K., 1972. Filtering marine magnetic anomalies. *Journal of Geophysical Research* 77, 7089-7099.
- Shuhail, M., Yatheesh, V., Bhattacharya, G.C., Muller, R.D., Kamesh Raju, K.A., Mahender, K., 2018. Formation and evolution of the Chain-Kairali Escarpment and the Vishnu Fracture Zone in the Western Indian Ocean. *Journal of Asian Earth Sciences* 164, 307-321.

- Small, C., Cochran, J.R., Sempere, J-C., Christie, D., 1999. The structure and segmentation of the Southeast Indian Ridge. *Marine Geology* 161, 1-12.
- Storey, M., Mahoney, J.J., Saunders, A.D., Duncan, R.A., Kelley, S.P., Coffin, M. F., 1995. Timing of hotspot related volcanism and the breakup of Madagascar and India. *Science* 267, 259-271.
- Tapscott, C.R., Patriat, P., Fisher, R.L., Sclater, J.G., Hoskins, H., Parsons, B., 1980. The Indian Ocean triple junction. *Journal of Geophysical Research* 85, 4723-4739.
- Tebbens, S.F., Cande, S.C., Kovacs, L., Parra, J.C., LaBrecque, J.L., Vergara, H., 1997. The Chile ridge: A tectonic framework. *Journal of Geophysical Research* 102, 12035-10259.
- Torsvik, T. H., Tucker, R. D., Ashwal, L. D., Eide, E. A., Rakotosolofa, N. A., de Wit, M. J., 1998. Late Cretaceous magmatism in Madagascar: Palaeomagnetic evidence for a stationary Marion hotspot. *Earth and Planetary Science Letters* 164, 221 – 232, doi:10.1016/S0012-821X(98)00206-4.
- Torsvik, T.H., Tucker, R.D., Ashwal, L.D., Carter, L.M., Jamtveit, B., Vidyadharan, K.T., Venkataramana, P., 2000. Late Cretaceous India-Madagascar fit and timing of breakup related magmatism. *Terra Nova* 12, 220-224.
- Torsvik, T. H., Amundsen, H., Hartz, E.H., Corfu, F., Kuszniir, N., Gaina, C., Doubrovine, P.V., Steinberger, B., Ashwal, L.D., Jamtveit, B., 2013. A Precambrian microcontinent in the Indian Ocean. *Nature Geoscience* doi: 10.1038/NGEO1736
- Weissel, J.K., Anderson, R.N., Geller, C.A., 1980. Deformation of the Indo-Australian plate. *Nature* 287, 284-291.
- Wessel, P. Smith, W. H. F., 1998. New improved version of Generic Mapping Tools released. *EOS Transactions, American Geophysical Union* 79, 579.
- Wessel, P., Matthews, K.J., Muller, R.D., Mazzoni, A., Whittaker, J.M., Myhill, R., Chandler, M.T., 2015. Semi automatic fracture zone tracking. *Geochemistry Geophysics Geosystems* doi: 10.1002/2015GC005853.
- Whittaker, J.M., Afonso, J.C., Masterton, S., Muller, R.D., Wessel, P., Williams, S.E., Seton, M., 2015. Long-term interaction between mid-ocean ridges and mantle plumes. *Nature Geoscience* doi: 10.1038/NGEO2437.
- Zhang T, Lin J, Gao J Y. 2011. Interactions between hotspots and the Southwest Indian Ridge during the last 90 Ma: Implications on the formation of oceanic plateaus and intra-plate seamounts. *Science China Earth Sciences* 54, 1177–1188, doi: 10.1007/s11430-011-4219-9.

Figure Captions

Figure 1: Bathymetric map of the Indian Ocean (Amante and Eakins, 2009) depicting the major tectonic elements. Large igneous provinces are marked as thin red outlines (Coffin and Eldholm, 1994). Present day mid-oceanic ridge system is marked as a thick black outline. Fracture zones (thin black dashed lines) are from Matthews et al. (2016a), and magnetic anomalies (thin black continuous lines) are from Royer et al. (1989). The trace of the Rodriguez Triple Junction (RTJ) on the three plates is marked as thick pink dashed lines (Patriat and Segoufin, 1988). The deformation zone in the Indian Ocean is marked as a thick dashed brown outline (Gordon et al., 1998). The study area is shown as a black rectangle. CbR: Carlsberg Ridge; CIR: Central Indian Ridge; CLR: Chagos Laccadive Ridge; CoR: Comorin Ridge; CB: Crozet Bank; Laccadive Basin; LB; MhFZ: Mahanoro FZ; MAM: Mammerickx microplate; MFZ: Mauritius FZ; MP: Madagascar Plateau; NAFZ: Northern Astrolabe FZ; NBFZ: Northern Boussole FZ; NER: Ninetyeast Ridge; SAFZ: Southern Astrolabe FZ; SBFZ: Southern Boussole FZ; SEIR: Southeast Indian Ridge; SL: Sri Lanka; SWIR: Southwest Indian Ridge. VFZ: Vishnu FZ.

Figure 2: Magnetic tracks (Table 1) used in the present study superimposed on the satellite gravity mosaic (Sandwell et al., 2014). DSDP/ODP sites which reached basement are shown as black stars with maximum age in parentheses, while those which did not reach basement are shown as black squares. The trace of the RTJ published earlier is shown as a thick red dashed line (Patriat and Segoufin, 1988; Dymant, 1993) and a thick blue dashed line (Cande et al., 2010). The deformation zone in the Indian Ocean is marked as a thick dashed brown outline (Gordon et al., 1998). Large igneous provinces are marked as red outlines (Coffin and Eldholm, 1994). The black rectangle marks the portion of the study area depicted in figure 6. CLR: Chagos Laccadive Ridge; CoR: Comorin Ridge; LB: Laccadive Basin.

Figure 3: Magnetic profiles inmd (eastern) and f6 (western) plotted along with the synthetic seafloor spreading models (red). Ship-borne bathymetry is shown in blue. Half-spreading rates are in mm/yr. The ages of the chrons identified in the present study are given in table 2. Magnetic anomalies are identified using the Gee and Kent (2007) geomagnetic polarity time scale. Spreading parameters are given in table 3.

Figure 4: Magnetic anomalies identified in the present study are marked in different colours on the stacked magnetic profiles. Ship-borne bathymetry wherever available is shown in blue. RTJ trace older to C29o by Patriat and Segoufin (1988) and Cande et al. (2010) are shown as thick dashed red and blue outlines respectively. Distorted magnetic signatures are shaded in light green and blue, and described in text and figure 6. The magnetic signature around C32ay outlined in yellow is absent along profile rc1707. Thick dashed purple outline denotes the RTJ trace older to C29o inferred in this study. FZ: Fracture Zone.

Figure 5: The magnetic anomaly identifications made in the present study (filled symbols) are plotted along with published identifications (open symbols) as per legend (Desa et al., 2009; Cande et al., 2010; Cande and Patriat, 2015). The C33y and C32ay isochrons lying adjacent to each other along 3°S are encircled in red. Satellite-derived gravity is plotted in the background (Sandwell et al., 2014). Fracture zones are shown as black dashed lines (Matthews et al., 2016a). The extent of the large igneous provinces is shown as a thin red outline (Coffin and Eldholm, 1994). The deformation zone in the Indian Ocean is marked as a thick dashed brown outline (Gordon et al., 1998). CLR: Chagos Laccadive Ridge; CoR: Comorin Ridge; IFZ: Indira FZ; NAFZ: Northern Astrolabe FZ; NBFZ: Northern Boussole FZ; VFZ: Vishnu FZ.

Figure 6(a): Composite plot of satellite-derived gravity (red), magnetics (black) and ship-borne bathymetry if available (blue), along portions of selected profiles (enclosed in a rectangle in figure 2) plotted in figure 6b. These profiles depict distorted magnetic signatures with respect to

the easternmost profile ‘inmd’ of the study area. The seafloor spreading model is shown along this profile. Symmetric magnetic anomalies (marked as red dashed line and rectangles) about a central anomaly associated with a gravity low indicate an extinct spreading ridge (thick black dashed line) and extra crust (light green shade). Distorted magnetic anomalies representing a rotated block are shaded light blue.

Figure 6(b): Satellite-derived free-air gravity mosaic of the western portion of the study area (enclosed in rectangle in figure 2), where the geophysical signatures are distorted. The profiles depicting the distorted signatures are analysed in figure 6a. A zone of up to 220 km E-W and 120 km N-S extent has been identified as the transferred crust (black dashed outline). To its south, a 180 km diameter zone (blue dashed outlines) depicting circular trends and distorted magnetic signature is distinct and represents a rotated microplate. Remaining information as in Figure 5.

Figure 7: The rotation poles inferred in this study (with and without deformation) are plotted along with the published poles as per legend, for chrons: C34y, C33y, C31y and C29o (Tables 4 and 5). Antarctica is kept in its present-day position.

- (a) India-Antarctica rotation
- (b) Africa-Antarctica rotation

Figure 8: Plate reconstruction models generated using GPlates (Boyden et al., 2011) for different chrons. Rotation parameters are provided in table 5 with Antarctica in its present-day position. The active spreading ridge system (thin pink dashed outline) consists of the SWIR separating Africa from Antarctica, the SEIR separating India from Antarctica, and the MR separating Africa from India. Fracture zones are marked as black dashed lines (Matthews et al., 2016a). Magnetic picks are marked in different symbols (as per age) and in different colors (as per the plate of present-day location), as stated in the legend. Predicted/synthetic isochrons on the African and Antarctic plates are shown as thin blue dashed lines. The RTJ trace on all the three plates is marked in green. Marion hotspot location is marked as a yellow diamond. On the Indian plate, the transferred crust is marked in orange, while the microplate in brown. 86FZ: 86°E FZ; AFZ: Astrolabe FZ; BFZ: Boussole FZ; CB: Crozet Bank; CoR: Comorin Ridge; CR: Conrad Rise; I: India; KFZ: Kerguelen FZ; M: Madagascar; MFZ: Mauritius FZ; MhFZ: Mahanoro FZ; MP: Madagascar Plateau; SL: Sri Lanka; VFZ: Vishnu FZ.

- (a) C34y: The RTJ is located north of the Conrad Rise, at the southwestern tip of the Comorin Ridge. The northern portion of the Madagascar Plateau is emplaced by this time, and its eastern edge appears to act a transform fault between the C34y picks off Madagascar and western CIOB.
- (b) C33y: The RTJ has left a linear trace on the India and Antarctic plates. The trace trends eastward on the African plate. Here the Vishnu FZ is the active transform fault joining the C33y picks off Madagascar and western CIOB. Orthogonal spreading is observed along the SWIR.
- (c) C31y: The RTJ has moved more westward due to northwest propagation of the SWIR. The Marion hotspot is now in close vicinity of the RTJ and SWIR. The model depicts that the transfer of extra crust inferred in the study area has taken place by this time. On the Antarctic plate, the RTJ probably traces a circular path around the Crozet Bank which is emplaced by this time. A large amount of crust including the older RTJ trace is transferred from the African to the Antarctic plate. Counter clockwise rotation of the SWIR FZs is observed in the reconstruction. The conjugate Vishnu and Mauritius FZs are active by this time.

(d) C29o: The SWIR is propagating eastward and so is the RTJ, causing the formation and rotation of a microplate in the study area. The counter clockwise rotation of the SWIR fracture zones is seen continuing. The Boussole FZ is also active now. The Marion hotspot activity causes overprinting the older magnetic chrons.

Figure 9: Satellite gravity maps (Sandwell et al., 2014) on which the RTJ traces prior to C29o inferred in the present study are plotted. The published RTJ traces are shown as a thin red dashed line (Patriat and Segoufin, 1988; Dyment, 1993) and thin blue dashed line (Cande et al., 2010). The magnetic anomaly identifications, the large igneous provinces and fracture zones are as in figure 5.

(a) The CIOB: The RTJ trace inferred in this study is shown as a purple dashed outline. It almost agrees with that of Patriat and Segoufin (1988) and Dyment (1993). The transferred crust and the rotated microplate are shown as thick dashed black and pink outlines respectively.

(b) The SWIR: The inferred RTJ trace south of SWIR (on the Antarctic plate) is marked in thick blue dashed outline, while the African trace is marked in purple dashed outline. These traces match well with the published trace (Patriat and Segoufin, 1988) on the African plate between C31y and C29o, while on the Antarctic plate there is a minor mismatch. The older African trace is inferred on the Antarctic plate. The extinct spreading ridge inferred by Whittaker et al. (2015) is marked as a thick black dashed outline. The Crozet Bank (CB) is seen enclosed by the circular RTJ trace between C33y and C31y. DCR: Del Cano Rise; MP: Madagascar Plateau; SWIR: Southwest Indian Ridge.

List of Tables

Table 1: Magnetic dataset used in the present study. NCEI: National Centers for Environmental Information, Colorado

Table 2: Ages of magnetic anomalies used in the present study (Gee and Kent, 2007)

Table 3: Parameters used for generation of synthetic seafloor spreading model

Table 4: Rotation pole parameters inferred from the magnetic picks used in the present study. Antarctica is kept in its present-day position. Clockwise rotation is signed negative. These pole parameters are plotted in figure 7.

Table 5: Table listing the rotation poles inferred in the present study after incorporating the deformation effect, and some published poles. Antarctica is kept in its present-day position. These poles are plotted in figure 7.

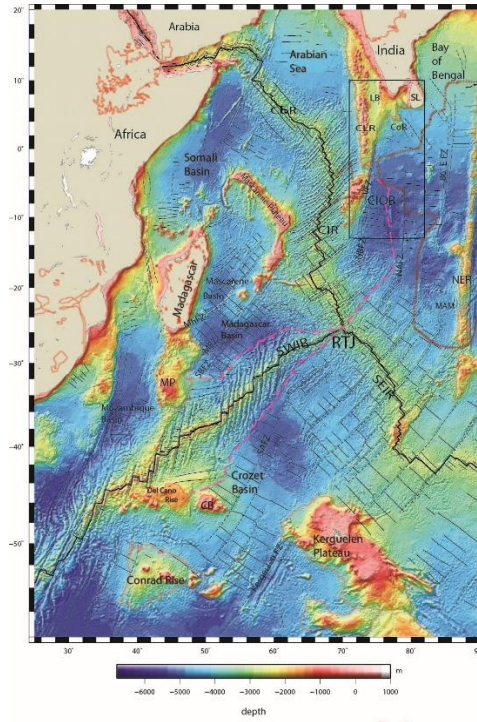


Figure 1

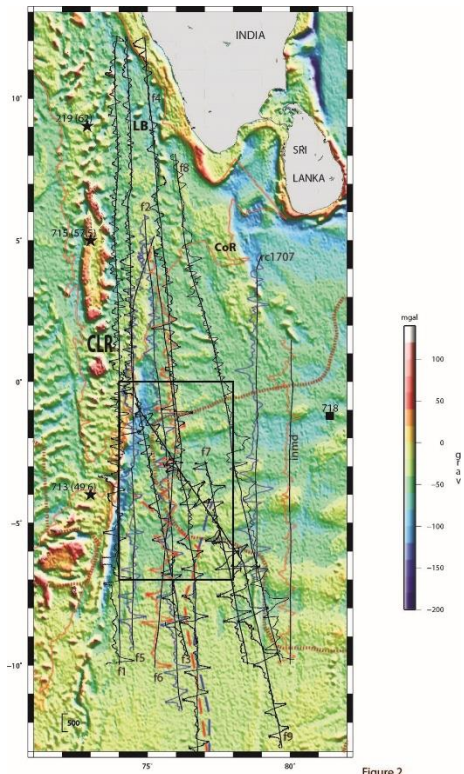


Figure 2

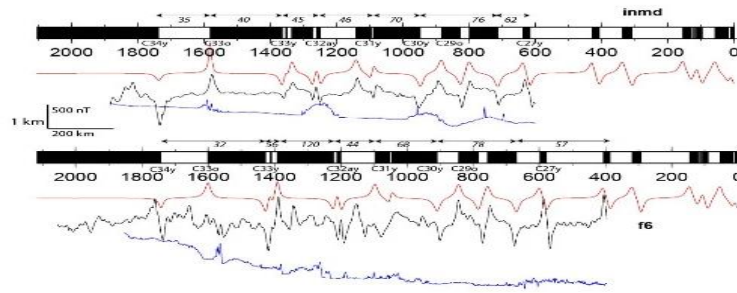


Fig. 3

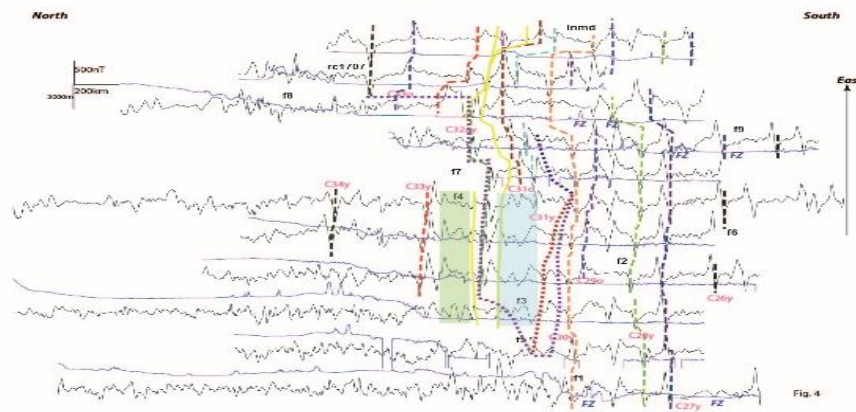


Fig. 4

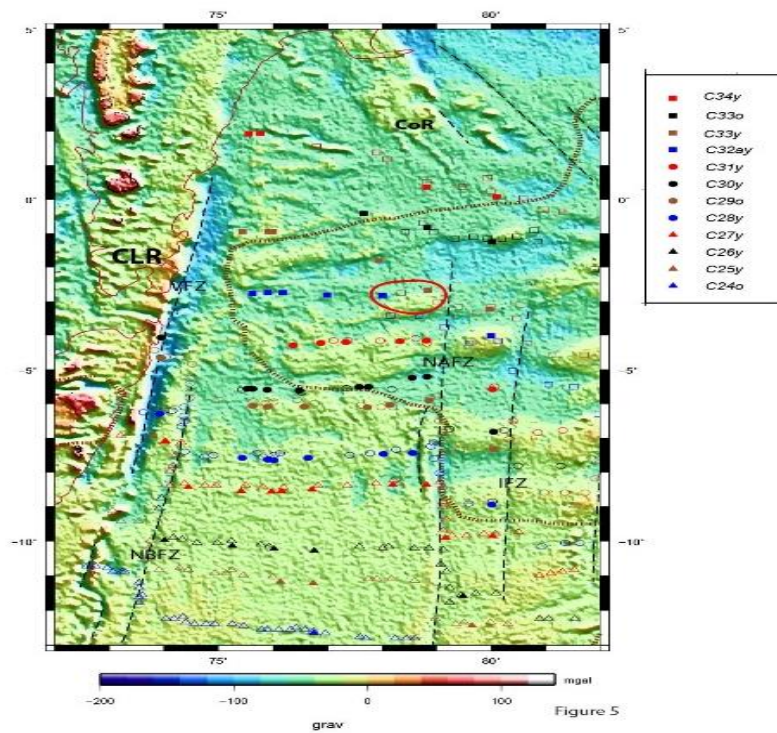


Figure 5

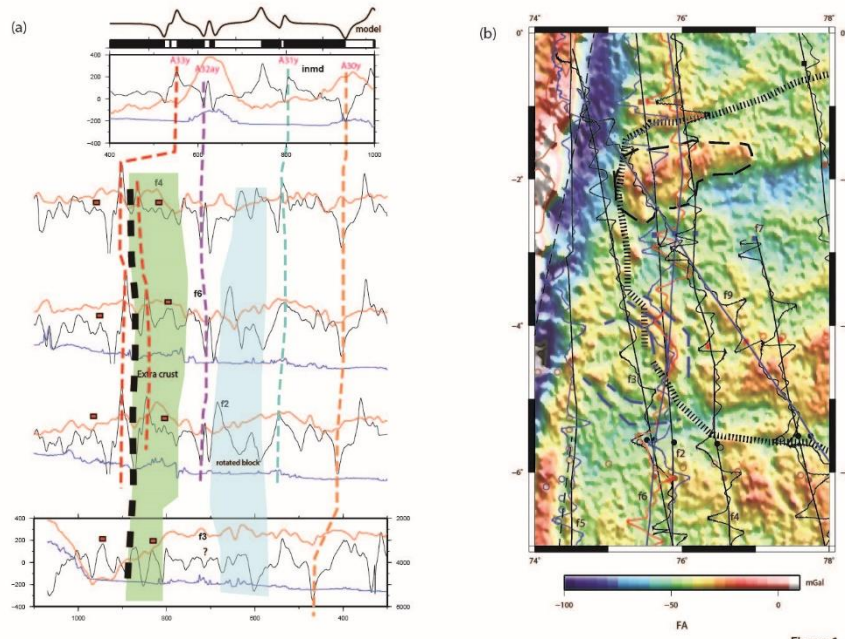


Figure 6

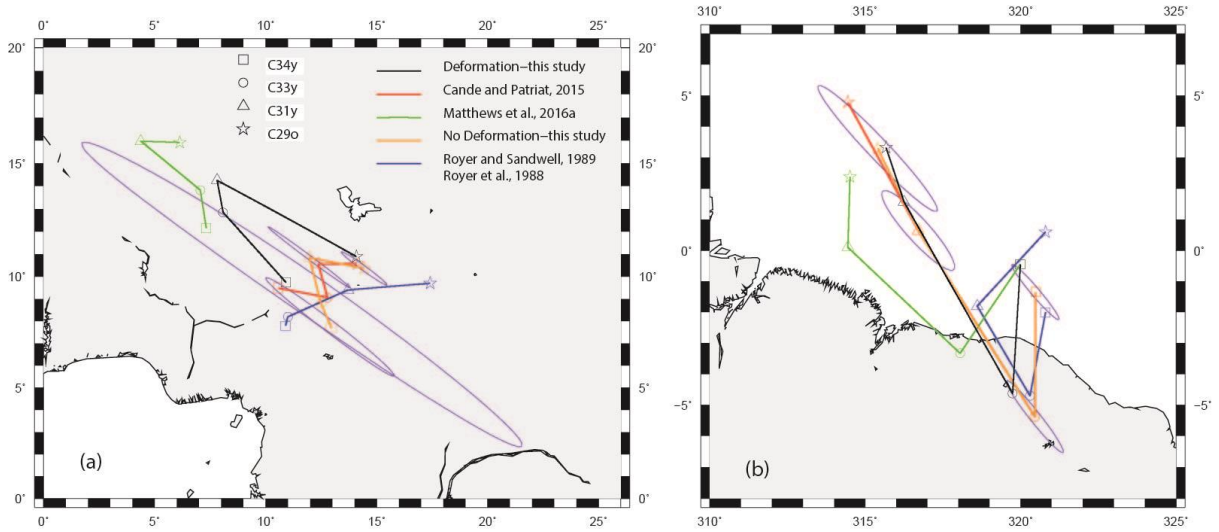


Figure 7

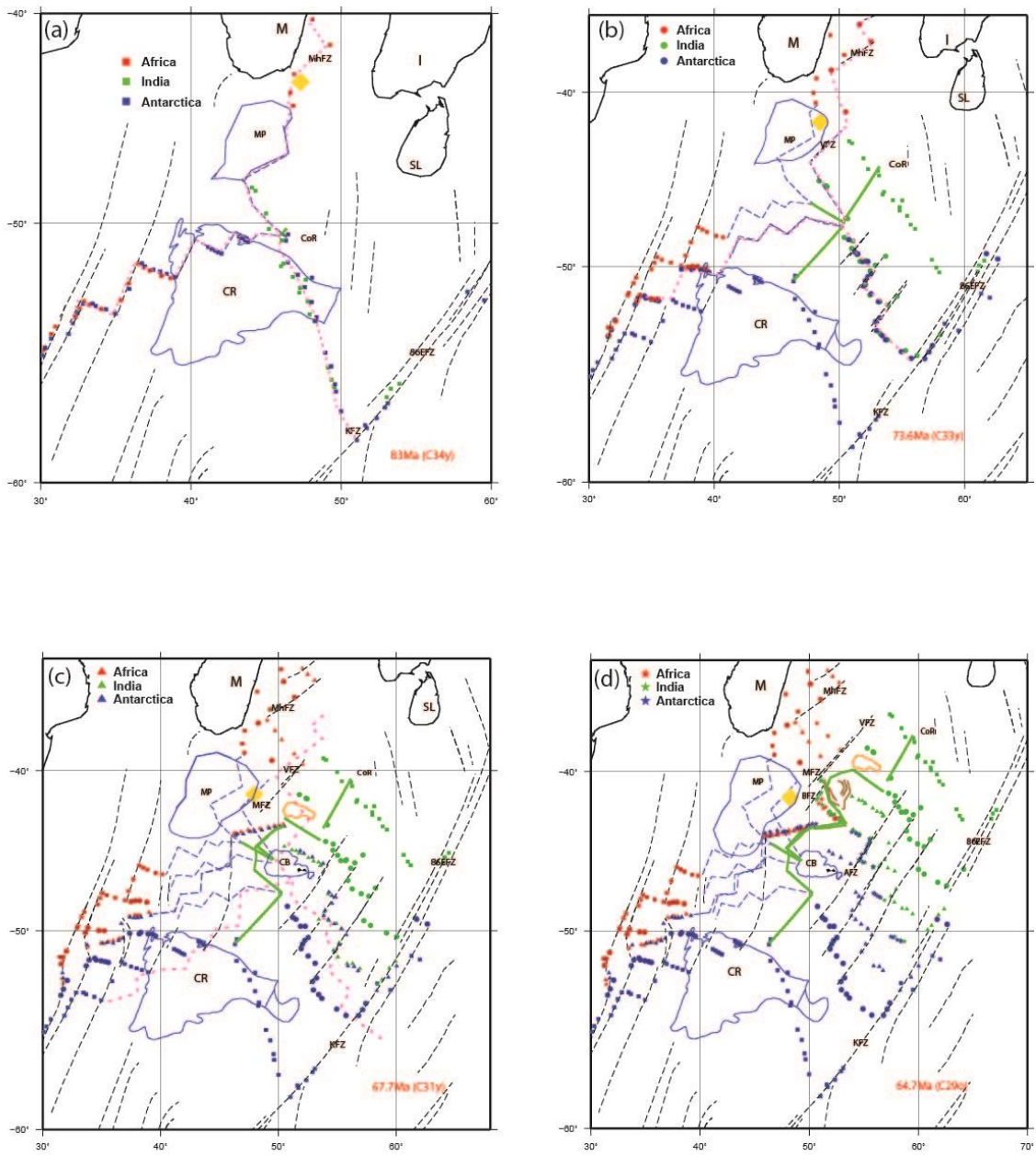


Figure 8

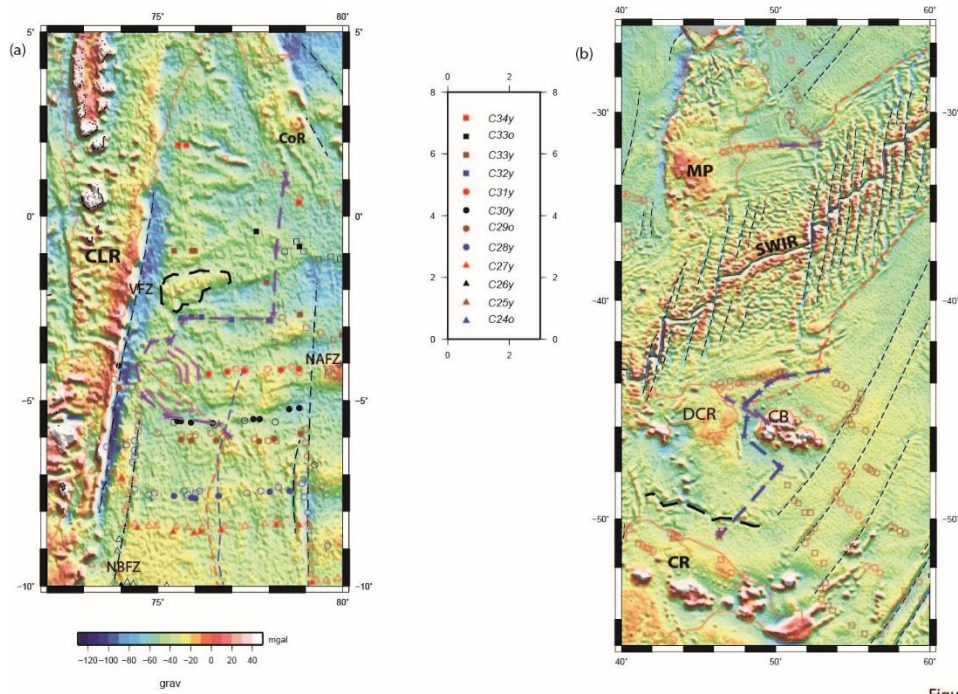


Figure 9

Table 1: Magnetic dataset used in the present study. NCEI: National Centers for Environmental Information, Colorado

Sr. no.	Profile name	Length (km)	Source
1	f1	2456	This study
2	f2	1942	
3	f3	2440	
4	f4	2933	
5	f5	1639	
6	f6	1658	
7	f7	814	
8	f8	2037	
9	f9	1485	
10	inmd	1313	NCEI
11	rc1707	1285	
	Total	20000	

Table 2: Ages of magnetic anomalies used in the present study (Gee and Kent, 2007)

Chron	Age in Ma
C24o	53.35
C25y	55.90
C26y	57.55
C27y	60.92
C28y	62.50
C29o	64.75
C30y	65.58
C31y	67.74
C31o	68.74
C32ay	71.59
C33y	73.62
C33o	79.08
C34y	83.00

Table 3: Parameters used for generation of synthetic seafloor spreading model

Parameter	Value
Spreading direction	0°
Thickness of magnetized layer	0.5 km
Susceptibility (cgs units)	0.05
palaeolatitude	-40°
Present day inclination	-23.83
Present day declination	-5.52
Formation strike	10°

Table 4: Rotation pole parameters inferred from the magnetic picks used in the present study.

Antarctica is kept in its present day position. Clockwise rotation is signed negative.

Notes: *a, b, c, d, e,* and *f* are covariances and have units of 10^{-7} radians². Covariance matrices are reconstructed from the equation

Africa-Antarctica												
Anomaly	Lat (N)	Long (E)	Angle	k	a	b	c	d	e	f	points	segments
C34y	-1.35	-39.52	17.82	0.5	5.97	3.19	2.08	-10.07	-5.63	18.21	122	10
C33y	-5.38	-39.54	13.91	0.94	12.38	5.22	3.21	-19.64	-9.15	33.9	67	9
C31y	0.641	-43.29	11.98	0.33	4.04	2.61	2.28	-5.82	-3.96	10.15	95	12
C29o	3.3	-44.6	11.69	0.61	11.8	12.98	15.56	-22.3	-25.35	45.24	74	10
India-Antarctica												
Anom	Lat(N)	Long(E)	angle	k	a	b	c	d	e	f	points	seg
C34y	7.7	12.97	-65.05	0.07	64.6	66.7	73.2	-133.8	-141.5	281.2	40	4
C33y	8.81	12.49	-56.42	0.027	182.7	251.4	352.8	-376.7	-519.2	785.0	37	6
C31y	10.85	11.97	-51.13	0.38	83.05	115.1	161.6	-166.8	-232.9	338.4	63	7
C29o	10.36	14.45	-47.95	0.96	54.71	82.13	126.2	-103.4	-155.6	198.5	34	5

$$1/k \times \begin{pmatrix} a & b & d \\ b & c & e \\ d & e & f \end{pmatrix}$$

Table 5: Table listing the rotation poles computed after incorporating the deformation effect (this study) and some published poles.

Antarctica is kept in its present day position. These poles are plotted in figure 7.

Chron	Plate ID/Plate	Latitude	Longitude	Angle	Source	
C34y	501 India	9.74	10.92	-63.89	Present study with deformation effect	
	701 Africa	-0.45	-40.01	17.77		
C33y	501 India	12.85	8.08	-53.79		
	701 Africa	-4.63	-40.26	13.83		
C31y	501 India	14.26	7.81	-48.86		
	701 Africa	1.57	-43.75	11.91		
C29o	501 India	10.89	14.09	-46.82		
	701 Africa	3.33	-44.33	11.99		
C34y	501 India	12.15	7.33	-62.94		Matthews et al., (2016a) with deformation effect
	701 Africa	-0.45	-40.01	17.77		
C33y	501 India	13.83	7.06	-53.49		
	701 Africa	-3.33	-41.95	13.53		
C31y	501 India	15.97	4.38	-48.13		
	701 Africa	0.1	-45.56	11.7		
C29o	501 India	15.92	6.13	-44.04		
	701 Africa	2.38	-45.49	11.36		
C34y	501 India	9.49	10.56	-63.88	Cande and Patriat, (2015) Without deformation effect	
	701 Africa	-1.35	-39.52	17.82		
C33y	501 India	9.07	12.79	-56.56		
	701 Africa	-5.38	-39.54	13.91		
C31y	501 India	10.56	12.37	-51.26		

	d701 Africa	0.64	-43.29	11.98	
C29o	501 India	10.57	14.13	-47.84	SWIR FZ Basic model Both from (Cande et al., 2010)
	701 Africa	4.79	-45.56	-11.70	
		1.82	-39.51	-11.68	
C34y	501 India	7.8	10.9	-65.1	Royer and Sandwell (1989) Royer et al., (1988)
	701 Africa	-2.0	-39.2	17.85	Without deformation effect
C33y	501 India	8.2	11.0	-62.18	
	701 Africa	- 4.7	-39.7	16.04	
C31y	501 India	9.4	13.7	-51.59	
	701 Africa	-1.8	-41.4	13.47	
C29o	501 India	9.7	17.4	-45.12	
	701 Africa	0.6	-39.2	11.32	